Genetic variants of *Tgfb1* act as context-dependent modifiers of mouse skin tumor susceptibility

Jian-Hua Mao*, Elise F. Saunier*, John P. de Koning*†, Margaret M. McKinnon*, Mamie Nakijama Higgins*, Kathy Nicklas*, Hai-Tao Yang*, Allan Balmain*‡§, and Rosemary J. Akhurst*§¶‖

*Cancer Research Institute, Comprehensive Cancer Center, Departments of ‡Biochemistry and ¶Anatomy, and §Program in Human Genetics, University of California, San Francisco, CA 94143-0875

Communicated by James E. Cleaver, University of California, San Francisco, CA, April 4, 2006 (received for review November 28, 2005)

The human *TGFB1* gene is polymorphic, and genetic variants are associated with altered cancer risk. However, human genetic association studies have had variable outcomes because TGFβ1 action is context-dependent. We used the murine skin model of chemical carcinogenesis in genetic linkage analysis of three independent *Mus musculus* NIH/Ola × (*Mus spretus* × *M. musculus* NIH/Ola)F_1 backcrosses, to identify a skin tumor susceptibility locus, *Skts14*, on proximal chromosome 7. *Tgfb1* maps at the peak of linkage. The mouse *Tgfb1* gene is polymorphic, resulting in cis-regulated differential allelic mRNA expression between *M. spretus* and *M. musculus* in F_1 mouse skin. This phenomenon is reflected in differential phospho-SMAD2 levels, downstream of TGFβ signaling, between these two mouse species. In normal F_1 mouse skin, the $Tgfb1^{SPR}$ allele is expressed at higher levels than the $Tgfb1^{NIH}$ allele, and this differential is accentuated by phorbol 12-myristate 13-acetate treatment. In benign F_1 papillomas, this imbalance is reversed, possibly by selection against expression of a hyperactive $Tgfb1^{SPR}$ allele in TGFβ growth-responsive tumors. We demonstrate that skin tumor susceptibility is altered by *Tgfb1* gene dosage, but that manifestation of *Tgfb1*-linked skin tumor susceptibility in *M. musculus* NIH/Ola × (*M. spretus* × *M. musculus* NIH/Ola)F_1 backcross mice depends on interactions with another unlinked tumor modifying locus, *Skts15*, that overlaps *Tgfbm3* on chromosome 12. These findings illustrate the power of complex genetic interactions in determining disease outcome and have major implications to the assessment of disease risk in individuals harboring variant *TGFB1* alleles.

carcinoma | chemical skin carcinogenesis | genetic interaction | TGFβ

TGFβ acts as a negative growth regulator of normal and benign proliferative epithelial cells (1–3), but stimulates tumor progression once accumulation of oncogenic mutations dampens the tumor's negative growth response to TGFβ (4–6). Additionally, TGFβ overproduced by both the malignant cell and tumor stroma may act on the tumor microenvironment to indirectly stimulate tumor progression (7, 8). TGFβ alters stromal cell characteristics, such as extracellular matrix deposition, secretion of proteases and other cytokines that enhance angiogenesis, and tumor growth and plasticity (9, 10). Moreover, it can act as a very potent local and systemic immunosuppressor (11–13).

Genes encoding components of the TGFβ1-signaling pathway, including *TGFB1* (14) and *TGFBRI* (15, 16), have been shown to be functionally polymorphic in humans, and genetic associations have been found between carriers of specific *TGFB1* and *TGFBR1* polymorphic variants and cancer susceptibility (15–20). The *TGFB1* gene harbors polymorphisms in its promoter, plus amino acid polymorphisms in its signal peptide that influence protein secretion and levels of freely circulating TGFβ1 (14, 21–23). Several independent groups have demonstrated a genetic association between variant *TGFB1* alleles and altered risk for breast cancer (17, 19, 20, 24). The most extensive report was that of a case-control study of >3,900 early-onset (median age 50) invasive breast cancer patients and a similar number of controls (17). Dunning *et al.* (17) demonstrated that homozygosity for the high expressing $TGFB1^{Pro\text{-}10}$ allele was associated with an increased invasive cancer risk (odds ratio 1.25), which would support a positive role of *TGFB1* in tumor progression. Conversely, in a cohort study of >3,000 women >65 years old at recruitment, of which 146 developed breast cancer over the following 9 years, it was found that women homozygous for the high-expressing $TGFB1^{Pro\text{-}10}$ allele were at a reduced risk of developing breast cancer, suggesting that *TGFβ1* has breast tumor-suppressing activity in this cohort (19). One explanation for these seemingly discrepant findings is ascertainment bias in selecting only young women with invasive breast cancer (17) vs. women who had reached 65 years of age cancer-free (19). Taken together, these studies support the model of the dual role of TGFβ in tumorigenesis (4). They illustrate that the prediction of cancer risk associated with a particular *TGFB1* allele depends on interacting genetic and environmental factors such that the hyperactive *TGFB1* allele may confer either cancer protection or increased risk. This thesis was recently substantiated by the studies of Shin *et al.* (24) which emphasize the importance of understanding the context-dependent action of TGFβ1 and hint at the importance of genes that interact with *TGFB1* in determining disease risk. Similar conclusions were recently made for risk of invasive prostate cancer (18).

In the current study, we demonstrate the existence of another skin tumor susceptibility locus, *Skts14*, containing the *Tgfb1* gene on proximal chromosome 7. We show that cis-acting regulatory elements of the mouse *Tgfb1* gene are polymorphic, leading to allelic mRNA expression, which could account for altered tumor susceptibility between mouse strains. Importantly, we demonstrate that the outcome of *Tgfb1* allelic variation depends on genetic context, particularly with respect to another modifier locus, *Skts15*, on chromosome 12 with which *Tgfb1* interacts.

Results

***Skts14*, a Skin Papilloma Susceptibility Locus on Proximal Mouse Chromosome 7.** Previous studies demonstrated the existence of a skin tumor susceptibility locus, *Skts1*, on proximal chromosome 7 that controls papilloma development (25). This linkage was originally mapped at a low resolution with a peak located at ≈50 Mb. In the current study, a panel of markers mapping at a higher resolution was used to regenotype the chromosome 7-linkage region in 306 (NIH/Ola × outbred *Mus spretus*)F_1 × NIH/Ola (NSP) backcross animals, revealing two linkage peaks and suggesting two distinct loci, with a more proximal locus, *Skts14*, mapping at ≈14 Mb on chromosome 7 (Fig. 1).

Conflict of interest statement: No conflicts declared.

Abbreviations: NSP, (NIH/Ola × outbred *M. spretus*) × NIH/Ola backcross; PMA, phorbol 12-myristate 13-acetate; LOD, logarithm of the odds; ΔCT, differential between threshold cycles.

†Present address: Semaia Pharmaceuticals, Buntlaan 44, 3971 JD, Driebergen, The Netherlands.

‖To whom correspondence should be addressed. E-mail: rakhurst@cc.ucsf.edu.

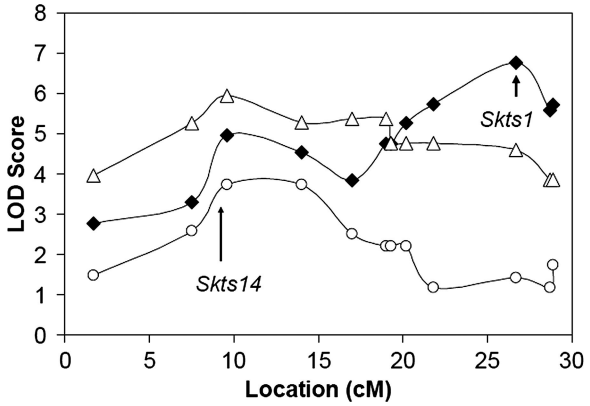

Fig. 1. *Skts14*, a skin tumor susceptibility locus on proximal mouse chromosome 7. LOD scores for genetic linkage on chromosome 7 in the F_1 NSP backcross ($n = 206$; ◆), and in that subset of the NSP backcross sharing Haplotype 4 ($n = 44$; ○). Also shown is a linkage analysis in the N_4 backcross ($n = 76$; △).

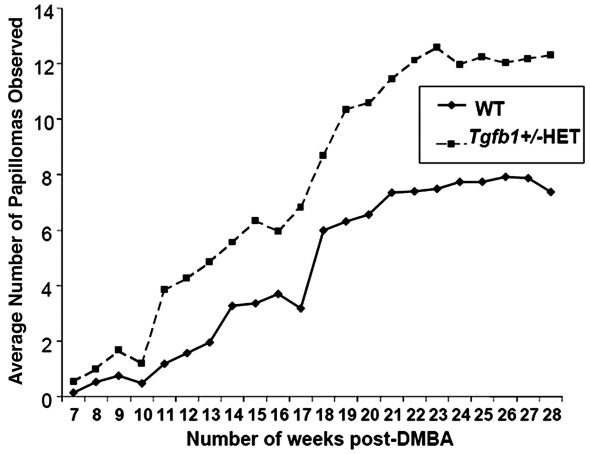

Fig. 2. Haploinsufficiency for *Tgfb1* increases papilloma incidence. Twenty-three WT and 30 *Tgfb1*+/− age-matched adult female mice were subjected to a standard chemical carcinogenesis protocol, and papilloma numbers were counted weekly. *Tgfb1*+/− developed significantly more papillomas than *Tgfb1*+/+ mice ($P = 0.025$ at 20 weeks; Student's *t* test).

Information on shared haplotypes in outbred populations can be used to refine the locations of potential disease susceptibility genes (26). A haplotype map was previously constructed for chromosome 7 by using variation in microsatellite lengths between the *M. spretus* alleles in the outbred colony (26). Interestingly, when the linkage data were stratified according to *M. spretus* haplotype, it was found that mice from one haplotype, namely "Haplotype 4," showed linkage only to the *Skts14* locus, in the absence of linkage to the original, more distal, *Skts1* locus, thus demonstrating that the two chromosome 7 loci act independently (Fig. 1). *Skts14* was further validated by linkage analysis on N_4 backcross mice that had been backcrossed four more generations to the NIH strain while selecting for those with papilloma resistance at each generation (N_4 mice). The LOD_{MAX} at *Skts1* was less than $LOD_{MAX} - 1$ at *Skts14*, again suggesting independence of *Skts14* from *Skts1* (Fig. 1).

***Skts14*^{NIH}-Linked Tumor Susceptibility Depends on Genetic Interaction with *Skts15*^{NIH} on Chromosome 12.** Genetic interaction between *Skts1* and *Skts5* on chromosomes 7 and 12, respectively, has been shown (27). This interaction analysis was repeated by using the higher density marker set over chromosome 7 and three markers located at 17.7, 34.1, and 60.7 Mb on chromosome 12. Interestingly, two peaks of significant interaction were found (see Table 2, which is published as supporting information on the PNAS web site). As seen in ref. 27, *Skts1* on chromosome 7 at 39.3 Mb shows genetic interaction with *Skts5* on chromosome 12 at 34.1 Mb. Independently, *Skts14* on chromosome 7 at 14 Mb interacts strongly with another tumor susceptibility locus, *Skts15*, on chromosome 12 at 17.7 Mb. Conversely, interactions between *Skts14* and *Skts5* and between *Skts1* and *Skts15* were both insignificant (see Table 2), illustrating the independence of the two genetic interactions between chromosomes 7 and 12.

Table 1 shows that homozygosity for NIH alleles at *Skts14* and *Skts15* confers higher tumor susceptibility in two independent *M. spretus* × NIH backcrosses (Table 1). The presence of a single *M. spretus* allele at either of these interacting loci results in relative resistance to papilloma development, with additional *M. spretus* alleles (*Tgfb1*$^{Spr/NIH}$;*D12Nds11*$^{Spr/NIH}$) having little additional effect (Table 1). The *Skts1*/*Skts5* interaction also shows this effect, but only in the NSP cross (Table 1), emphasizing the independence of the two interactions and the importance of the *Skts14*/*Skts15* interaction.

Haploinsufficiency for *Tgfb1*, a Candidate Gene at *Skts14*, Increases Papilloma Incidence. *Tgfb1* is an excellent candidate as a tumor susceptibility gene at *Skts14*, especially in light of the evidence that human *TGFB1* is functionally polymorphic and alters risks for breast and prostate cancer (17–19). We previously showed that keratinocyte-targeted TGFβ1 gene expression in the chemically induced model of mouse skin carcinogenesis reduces papilloma outgrowth (4). Fig. 2 demonstrates that 7,12-dimethylbenz[*a*]anthracene (DMBA)/phorbol 12-myristate 13-acetate (PMA) treatment of *Tgfb1*+/− mice leads to a significant increase in papilloma incidence compared with control *Tgfb1*+/+ mice, demonstrating that global alterations in TGFβ1 levels also influence mouse skin tumor susceptibility.

Basal and PMA-Inducible Gene Expression Levels of *Tgfb1*^{Spr} in Skin Are Higher than Those of *Tgfb1*^{NIH}. The coding region of *Tgfb1* was sequenced in its entirety in *M. spretus* and in three strains of *Mus musculus* (NIH, 129, and C57). No amino acid differences were found between any of the strains, although several silent SNPs were detected.

Table 1. Homozygosity for NIH alleles at both *Tgfb1* and *D12Nds11* associates with increased papilloma yield per mouse

		D12Nds11					*D12Mit154*		
Experiment	*Tgfb1*	NS	NN	*P* value	Experiment	*D7Mit18*	NS	NN	*P* value
NSP	NS	2.52 ($n = 59$)	2.31 ($n = 81$)	2.2×10^{-4}	NSP	NS	1.87 ($n = 91$)	2.68 ($n = 79$)	$<10^{-16}$
	NN	2.48 ($n = 90$)	5.03 ($n = 96$)			NN	2.07 ($n = 69$)	5.94 ($n = 87$)	
NSE	NS	3.14 ($n = 22$)	3.84 ($n = 32$)	3.1×10^{-10}	NSE	NS	2.12 ($n = 25$)	4.32 ($n = 19$)	0.006
	NN	3.61 ($n = 28$)	10.83 ($n = 24$)			NN	5.09 ($n = 22$)	10.56 ($n = 27$)	

P values were determined by the *Kruskal*–Wallis test. N, NIH allele; S, *spretus* allele; NSP, F_1 (NIH/O1a × outbred *M. spretus*) × NIH/Ola; NSE, F_1 (NIH/Ola × inbred SEG/Pas) × NIH/Ola.

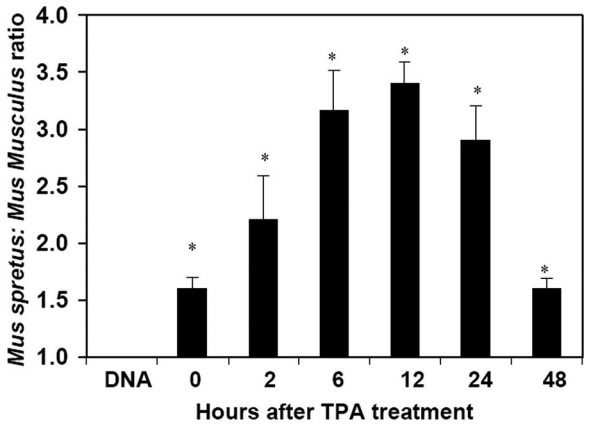

Fig. 3. Differential allelic expression of *Tgfb1* in normal mouse skin. RNA was prepared from normal skins of (NIH/Ola × SPRET/Gla)F_1 mice, untreated (0) or at various times (2, 6, 12, 24, or 48 h) after topical application of PMA. The *M. spretus* to *M. musculus Tgfb1* transcript ratio was determined by *TaqMan* analysis of cDNA by using allele-specific probes. All samples overexpressed the *M. spretus Tgfb1* allele, and this effect was accentuated 12 h after PMA treatment. For comparison, we also determined the *M. spretus*/*M. musculus* ratio in genomic DNA. As expected, this ratio is close to 1 for normal F_1 mice. Asterisks indicate significant differences between genomic DNA and cDNA samples. The means and standard deviations of three independent experiments are shown.

In the absence of TGFβ1 amino acid polymorphisms, functional polymorphism between the two mouse species could occur at the RNA level due to differential transcription, splicing, or message stability. To investigate this possibility, allele-specific *TaqMan* probes that distinguish between NIH/Ola and SPRET/Ei *Tgfb1* transcripts were designed on the basis of a silent SNP in the cDNA. Allele-specific expression patterns of *Tgfb1* were quantified within the skin of normal F_1 mice [(NIH/Ola × SPRET/Ei)F_1] at various times after topical treatment with PMA. *TaqMan* analyses of cDNA transcribed from RNA of normal mouse skin showed a significant and reproducible difference in basal *Tgfb1* gene expression of ≈1.7-fold in favor of the *M. spretus* allele (Fig. 3). This expression difference between the two alleles was enhanced after PMA treatment, reaching a maximum of a 3.5-fold differential at 12 h after PMA treatment (Fig. 3). In F_1 mice, both alleles of the *Tgfb1* gene are present within the same cell; thus, regulation of their differential expression must occur in cis. As a control, similar experiments using genomic DNA from the same F_1 hybrid mice invariably showed a 1:1 ratio by *TaqMan* analysis.

Sequencing of 5 kb of genomic DNA upstream from the translation initiation site, and the evolutionarily conserved first intron, revealed complete intraspecific conservation of *Tgfb1* within the *M. musculus* strains, but considerable interspecific polymorphism between *M. spretus* and *M. musculus*. Polymorphisms occur within the gene promoter, 5′ untranslated region of the mRNA and within the first intron, with some sequence variants altering potential transcription factor-binding sites, thus introducing the possibility of both transcriptional and posttranscriptional regulation of differential *Tgfb1* message levels between the two species (see Fig. 6, which is published as supporting information on the PNAS web site).

Reduced Basal Phospho-SMAD2 Levels in *M. musculus* Compared with *M. spretus* Epidermis. We investigated additional components of the TGFβ-signaling pathway downstream of TGFβ1 itself. Phosphorylation and nuclear translocation of the receptor-associated SMADs, SMAD2 and SMAD3, are early events in signal transduction downstream of the TGFβ receptor complex (5). To determine whether differential expression of the *Tgfb1* gene results in altered SMAD signaling between *M. spretus* and *M. musculus*, immunohistochemistry and Western blot analysis was performed to assess levels and localization of this marker of TGFβ signaling in WT *M. spretus* skin vs. WT and heterozygous *Tgfb1*+/− *M. musculus* skin. As predicted, heterozygous *Tgb1*+/− *M. musculus* epidermis had reduced levels of phospho-SMAD2 compared with *M. musculus* WT mice. Importantly, phospho-SMAD2 levels were greatly elevated in *M. spretus* compared with *M. musculus* epidermis (Fig. 4). Taken together, these results indicate that the TGFβ-signaling pathway is up-regulated substantially in cells and tissues from *M. spretus* mice.

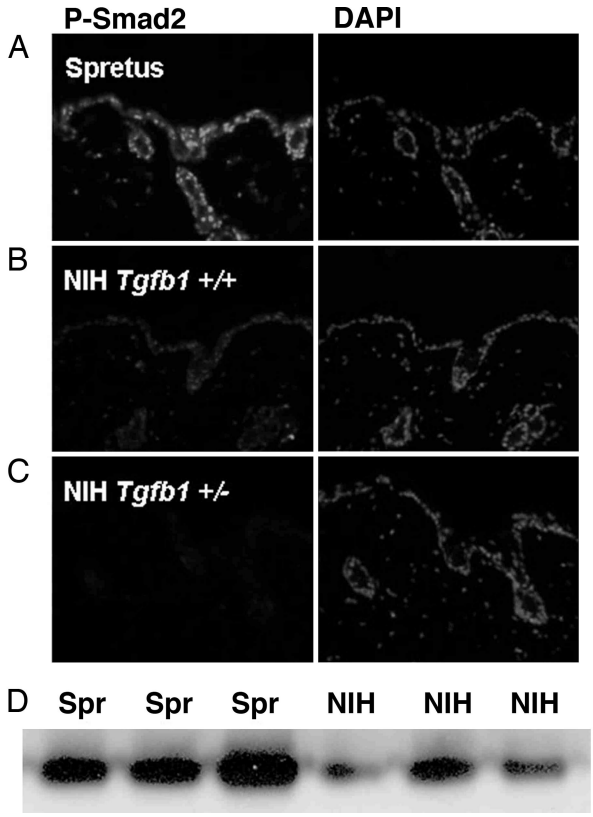

Fig. 4. Basal phospho-Smad2 levels are elevated in the skin of *M. spretus* compared with *M. musculus*. (*A–C*) Immunohistochemistry using an anti-phospho-SMAD2 antibody (that recognizes both phospho-Smad2 and phospho-Smad3) on untreated skins from *M. spretus* (*A*), *M. musculus Tgfb1*+/+ (*B*), and *Tgfb1*+/− (*C*) mice. (*D*) Different levels of phospho-SMAD2 were also observed by Western blot analysis. Cell lysates from three different *M. spretus* and three different *M. musculus* mice were immunoprecipitated with an anti-phospho-SMAD2-specific antibody, followed by Western blot analysis using the same antibody.

***Tgfb1*^{Spr} and *Tgfb1*^{NIH} Are Differentially Expressed in Tumor Cell Lines and Primary Papilloma.** It is widely accepted that mouse and human tumors have elevated expression of TGFβ1 (7, 28) that may ultimately favor malignant progression (9). The *Tgfb1* gene is autoinductive and up-regulated by ras via its AP-1-binding site (29, 30). Moreover, during multistage carcinogenesis in the mouse skin model, cytogenetic abnormalities accumulate and, at an early stage, tumor cells frequently show trisomy of chromosome 7 due to duplication of the chromosome harboring mutant H-ras. Subsequently, this chromosome may be further amplified and the chromosome bearing normal H-ras may also be lost (31, 32). The chromosomal imbalance involving chromosome 7 will also lead to duplication of *Tgfb1* in the proximal part of the

GENETICS

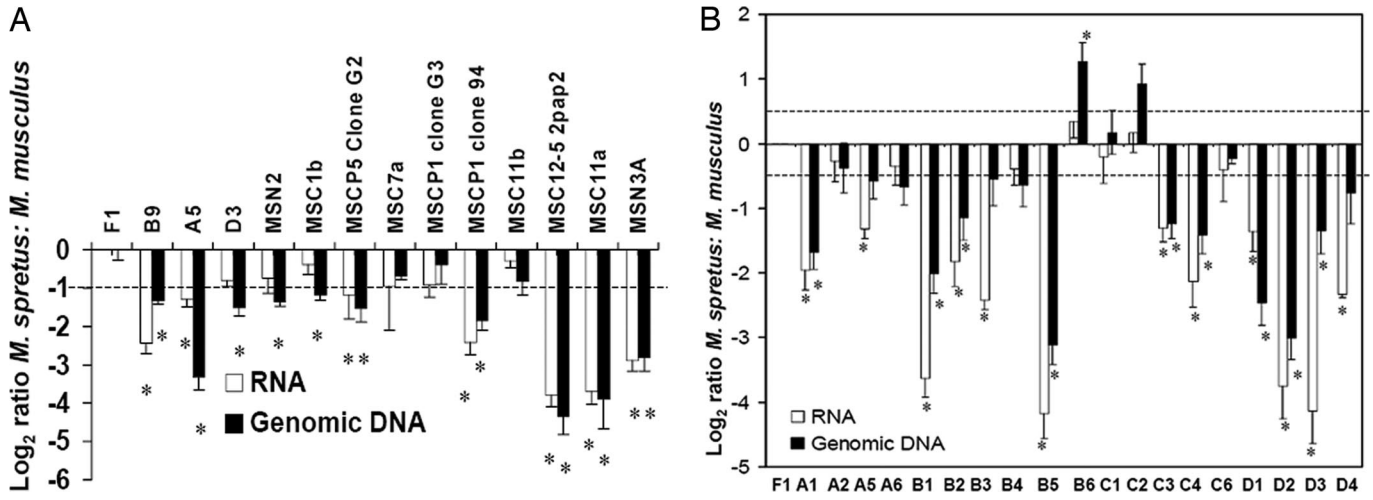

Fig. 5. Genomic imbalance and differential allelic expression of *Tgfb1* in tumors. (*A*) cDNA was prepared from skin tumor-derived *M. spretus*/*M. musculus* F_1 hybrid cell lines. Seven of these lines showed significant overexpression of the *M. musculus* allele, which is indicated by asterisks. Genomic DNA was isolated from the same samples, and *TaqMan* analysis was carried out to measure the relative copy number of different *Tgfb1* alleles. Ten of the samples (denoted by asterisks) showed significant amplification of the *M. musculus* allele of *Tgfb1*. (*B*) cDNA and genomic DNA was generated from primary papillomas of *M. musculus* NIH mice, congenic for *M. spretus* on proximal chromosome 7. *TaqMan* analysis was carried out as above. Nine tumors showed significant genomic imbalance at *Tgfb1* in favor of the *M. musculus* allele. These nine, together with an additional three had significant overexpression of $Tgfb1^{NIH}$, indicated by asterisks. Two tumors had genomic imbalance in favor of the *M. spretus* allele, but in both cases the $Tgfb1^{SPR}/Tgfb1^{NIH}$ expression ratio was not significantly different from 1.0. The dashed line in *A* and *B* denote the significance level for differential expression/genomic imbalance determined by Student's *t* test.

chromosome. Because duplication of the *M. spretus* allele would lead to very high levels of TGFβ signaling due to the endogenously high levels of the *Tgfb1 M. spretus* transcript (Fig. 3), it would be anticipated that there may be selection for duplication of the *M. musculus* chromosome during acquisition of trisomy. This selective trisomy would allow duplication of the mutant H-*ras* allele on distal chromosome 7 without causing major increases in expression levels of TGFβ1 in the proximal region. This hypothesis was verified by allele-specific *TaqMan* analysis of genomic DNA samples from 13 tumor cell lines derived from F_1 mice. Of these cell lines, 11 showed a genomic DNA imbalance in favor of the *M. musculus* chromosome, and *TaqMan* analysis demonstrated relatively reduced expression of the *M. spretus* $Tgfb1^{SPR}$ allele (Fig. 5*A*), despite the fact that the *M. spretus* allele is more highly expressed in normal skin (Fig. 3). We conclude that this reflects selection against the high level-expression of the *M. spretus Tgfb1* allele, which would tend to reduce growth of early stage primary tumors.

To exclude the possibility that preferential duplication of the *M. musculus* chromosome 7 is driven by an alternative tumor susceptibility locus, *Skts2*, which lies near the *H-ras* gene on distal chromosome 7 (25), we generated congenic mice containing only the proximal region (0–19 cM) of chromosome 7 from *M. spretus* on the NIH background. These animals are homozygous *M. musculus* in the distal portion of the chromosome containing the *H-ras* gene, and any preferential duplication of parental alleles cannot be driven by genes in the region of *Skts2.* As shown in Fig. 5*B*, 13 of 19 primary tumors examined had duplicated the *M. musculus* rather than the *M. spretus* chromosome 7 region containing *Tgfb1*, and these papillomas showed relative overexpression of the *M. musculus* compared with the *M. spretus Tgfb1* allele. Only two papillomas showed genomic overrepresentation of the *M. spretus Tgfb1* allele. In these two exceptional cases, the effects of genomic imbalance in favor of $Tgfb1^{Spr}$ were minimized at the RNA expression level of $Tgfb1^{Spr}$ compared with $Tgfb1^{NIH}$. This finding again supports the hypothesis of selection against $Tgfb1^{Spr}$ expression even in papillomas where the $Tgfb1^{Spr}$ allele is in excess (Fig. 5*B*; samples B6 and C2).

Discussion

It has been demonstrated that, genomewide, the strongest pairwise interaction between two genetic loci that modifies tumor susceptibility in the mouse skin model is between proximal chromosome 7 (*Skts1*) and proximal chromosome 12 (*Skts5*) (27). Fine genetic mapping now shows that *Skts1* and *Skts5* can each be dissected into two independently interacting regions of the genome. *Skts14* at 14.4 Mb on chromosome 7 interacts with *Skts15* at 17.7 Mb on chromosome 12 to drive papilloma susceptibility, and an equally strong interaction occurs between NIH alleles at *Skts1* at 39.3 Mb on chromosome 7 and *Skts5* at 34.1 Mb on chromosome 12. The LOD_{MAX} for *Skts14* is at *Tgfb1*, a very strong candidate gene for influencing cancer risk. Intriguingly, LOD_{MAX} for *Skts15* maps precisely at *Tgfbm3*, a locus previously identified by its ability to modify the phenotypic outcome of *Tgfb1* nullizygosity (33), giving indirect support to the concept that *Tgfb1* is the tumor modifier at 14.4 Mb at *Skts14*.

Unlike the situation for humans, there are no TGFβ1 amino acid polymorphisms between the different mouse strains examined. All strains encode the equivalent of the hyperactive signal peptide isoform observed in humans. Nevertheless, like the human gene, the mouse *Tgfb1* gene has a polymorphic gene promoter and 5′ noncoding region and drives differential expression of the two alleles in a cis-acting manner. In F_1 mouse skin, the *M. spretus Tgfb1* allele is expressed 1.7-fold higher than its *M. musculus* partner, and this differential is enhanced to nearly 4-fold after induction of the gene by PMA. Elevated ligand expression in *M. spretus* results in generalized up-regulation of basal TGFβ-signaling activity, as demonstrated by enhanced nuclear staining with a phospho-SMAD2 antibody in the epidermis. It would therefore appear that the hyperactive *M. spretus Tgfb1* allele is protective against tumor outgrowth due to the tumor-suppressing (growth inhibitory/differentiation-inducing) activity of TGFβ1 at early stages of tumor outgrowth (4, 34). It is therefore not surprising that this hyperactive *M. spretus* allele is selectively down-regulated either genetically and/or epigenetically in papillomas that are still growth-responsive to TGFβ. Indeed, selective loss of the *M. spretus* chromosome 7 in papillomas, which is frequently observed in F_1

and F_1 backcross mice (32), may indeed be driven, at least in part, by selection against the *M. spretus* hyperactive *Tgfb1* allele.

The tumor-protective role of the *M. spretus Tgfb1* allele is redundant if the animal possesses a *M. spretus* allele at *Skts15*. High tumor susceptibility is only seen in animals of the F_1 backcross that are homozygous NIH at both loci. A similar genetic interaction is seen regulating developmental angiogenesis in the mouse in which possession of NIH alleles at $Tgfbm3^{NIH}$ reduces the developmental dependence on TGFβ1 for normal angiogenesis (33). It is interesting that the same interacting loci, namely *Tgfb1* and *Skts15/Tgfbm3*, appear to alter susceptibility for both cancer and defective developmental angiogenesis. This phenomenon may be because the altered cancer risk seen here is related to alterations in angiogenic capacity or because this chromosome 7/12 interaction modifies fundamental processes in cell biology common to both tumorigenesis and angiogenesis and affecting several cell types (e.g., cell proliferation, survival, and migration). Indeed, the *Skts15/Tgfbm3* locus on chromosome 12 encompasses a small interval enriched in genes involved in regulation of cell proliferation, survival, and plasticity, including several genes known to be directly on the TGFβ-signaling pathway (33). *Tieg2b/Tieg3* is a TGFβ-inducible transcriptional repressor with antiproliferative and antiapoptotic functions (35). *Idb2* encodes Id2 (inhibitor of differentiation), which is also involved in transcriptional inhibitory responses to TGFβ (36–38) in cell growth control and angiogenesis (36, 37, 39, 40). Other genes involved in cell proliferation include *Ornithine decarboxylase* (*Odc*) and *Ribonucleotide reductase 2* (*Rrm2*), and those involved in modifying cellular plasticity and migration encode Rho kinase (*Rock2*), integrin β1-binding protein 1 (*Itgb1bp1/LCAP1*), and TNFα-converting enzyme (*Adam17*). It is possible that the gene, or combination of genes, at this locus responsible for *Tgfb1* developmental redundancy vs. $Tgfb1^{spr}$ redundancy for tumor resistance are different from each other. This theory remains to be tested. From the cancer perspective, it should be noted that a 2-Mb interval of the human genome syntenic to chromosome 12 at *D12Nds11* is amplified in >60% of human prostate tumors (41), a particularly provocative finding because the homozygous $TGFB1^{Pro\text{-}10}$ genotype in humans is associated with a 2.5-fold elevated risk of invasive prostate cancer (18).

The current study illustrates the importance of considering genetic context when undertaking human genetic association studies, particularly for genes that can have either positive or negative effects on disease progression. Indeed, despite highly significant genetic interaction between *Tgfb1* and *Skts15* ($P = 1.1 \times 10^{-8}$) in the *M. spretus* (*SEG/Pas*) × *NIH/Ola* backcross, neither of these loci reached significance when scored as independent quantitative trait loci ($P = 4.5 \times 10^{-3}$ for *Skts14* and $P = 3.4 \times 10^{-3}$ for *Skts15*). Thus, association of a single genetic polymorphism with potent phenotypic effects on disease risk may be masked by ignoring the contributions of interacting loci that either synergize or neutralize this genetic effect. The small 1.25-fold increase in relative risk for invasive breast cancer observed for homozygous $TGFB1^{Pro\text{-}10}$ individuals (17) may be an under estimate of *TGFB1*-associated cancer risk. The homozygous $TGFB1^{Pro\text{-}10}$ cohort may in fact be made up of a subpopulation of individuals in which $TGFB1^{Pro\text{-}10}$ elicits very high cancer risk (i.e., their genetic context favors tumor promoting activity of TGFβ1), and another subpopulation in which the risk is much smaller or even negative (19, 20) due to the protective effects of TGFβ1 in tumorigenesis. Indeed, this phenomenon could explain the discrepant *TGFB1* genetic association results seen in breast cancer for high-risk patients, namely those that develop breast cancer early in life (median age 50) (17) compared with those that have not developed cancer by age 65 (19). The discrepancy could also be due to definition of phenotypes. The studies of Dunning *et al.* (17) and Ewart-Toland *et al.* (18) focused on invasive cancer, whereas those of Ziv *et al.* (19) and Hishida *et al.* (20) did not distinguish between different cancer grades. Shin *et al.* (24) recently showed that high TGFβ1 levels may protect from low-grade cancer but predispose to invasive tumors. This type of effect has also been seen in cardiovascular disease whereby the hyperactive *TGFB1* allele has been associated with an increased risk of hypertension (14, 21) but, counterintuitively, with protection from myocardial infarction (14, 22). Such an effect could be because the prevalent TGFβ1 target cell differs for the two conditions. A similar complex interaction may well occur in cancer in which TGFβ has potent effects on both the tumor cell and on all cell types of the tumor microenvironment.

Many proteins have biphasic actions in tumorigenesis, such as c-myc and p53, which can act as either oncogenes or tumor suppressors, dependent on cellular context (42). The issue of epistasis is therefore very important in the design of human genetic association studies for estimating contributions to cancer risk. The elucidation of genetic networks of interacting genes will provide tools for a more holistic and combinatorial approach to accurate determination of disease risks in humans.

Materials and Methods

Animals and Tumor Induction. The mice used for these studies were described in refs. 25 and 27. Briefly, inbred NIH/Ola mice were purchased from Harlan Olac (Bicester, U.K). Outbred *M. spretus* and inbred SEG/Pas mice (derived from *M. spretus*) were obtained from S. Brown (Medical Research Council, Harwell, United Kingdom) and J.-L. Guenet (Institut Pasteur, Paris), respectively. SPRET/Ei mice were obtained from The Jackson Laboratory. *M. spretus* × NIH backcrosses were generated by breeding a male *M. spretus* to a female NIH mouse, and the female F_1 mice were backcrossed to male NIH. In the backcrosses, NSP, NSE [(NIH/Ola × inbred SEG/Pas) × NIH/Ola], and NSJ [(NIH/Ola × inbred SPRET/Ei) × NIH/Ola] breeding and tumor induction protocols were used as described in ref. 25, and papilloma susceptibility was estimated by the number of papillomas at 20 weeks after initiation. The phenotype data of 106 NSE, 162 NSJ, and 326 NSP animals were reported in refs. 25 and 27.

N_4 mice were generated by selecting a single mouse from the NSP backcross that developed no papillomas after chemical carcinogenesis treatment. The mouse was backcrossed through three generations onto the NIH strain, selecting another tumor-resistant mouse at each generation. At the N_3 generation, the "line" was expanded to generate 76 N_4 mice by backcrossing once more to the NIH strain. These mice were subjected to chemical carcinogenesis and genotyped across chromosome 7. Genetic linkage to tumor resistance was assessed by linear regression analysis using the SPSS statistics program (SPSS, Chicago).

Tgfb1+/− mice were on an NIH/Ola genetic background after backcrossing >10 generations These mice were subjected to the standard 7,12-dimethylbenz[*a*]anthracene/PMA chemical carcinogenesis protocol (25).

DNA Preparation, Genotyping, Linkage, and Haplotype Analysis. Genomic DNAs were prepared from tails and amplified by standard methods by using microsatellites. Negative binomial regression analysis was used to screen for predisposition loci and to identify interacting loci, as reported in ref. 27. For fine mapping of quantitative trait loci, we constructed haplotypes in outbred *M. spretus* mice for association studies by using the variation in length of microsatellites between the different NSP alleles.

Allele-Specific *TaqMan* Analysis. We measured allele-specific expression of *Tgfb1* using the ABI Prism 7700 Sequence Detection System (Applied Biosystems). PCR for allele-specific expression (50 μl) contained 50 ng of reverse-transcribed RNA or 50 ng of

GENETICS

genomic DNA, 1 × *TaqMan* universal PCR master mix, forward and reverse primers (900 nM), 200 nM VIC-labeled probe, and 200 nM FAM-labeled probe. Amplification conditions were as follows: 1 cycle of 50°C for 2 min, followed by 1 cycle of 95°C for 10 min, 40 cycles of 95°C for 15 s, and 60–64°C for 1 min. Completed PCRs were read on an ABI Prism 7700 Sequence Detector. PCR was done in triplicate for each sample, and experiments were repeated at least three times. ΔCT values were normalized to the average normal genomic ΔCT difference in each experiment. The ΔCT values between the two probes for the triplicates were then averaged. Probe specificity was assessed by analysis of pure *M. spretus* and pure *M. musculus* genomic DNAs as controls. ΔCT (CT difference between *M. spretus* and *M. musculus* probe) for pure *M. spretus* DNA was 16.1, and for pure *M. musculus* DNA it was −9.6.

Western Blotting Analysis. Total protein extracts were prepared from mouse skin with STEN lysis buffer (50 mM Tris, pH 7,4/2 mM EDTA/150 mM NaCl/1% Nonidet P-40/0.1% SDS/0.5% Triton X-100) containing Complete Protease Inhibitor mixture (CPI; Roche). Phospho-Smad2 protein was immunoprecipitated from 500 μg of total protein by using a rabbit anti-phospho-Smad2 antibody (a gift from J. Yingling, Eli Lilly) with 20 μl of protein G-Sepharose beads (GE Healthcare, Piscataway, NJ) at room temperature for 3–4 h. The antibody complexes were denaturated and separated by NuPAGE Novex PAGE (Invitrogen), transferred onto a poly(vinylidene difluoride) membrane (Millipore), and immunoblotted with the rabbit anti-phospho-Smad2 antibody. The membranes were washed and incubated with secondary horseradish peroxidase-conjugated antibody (Sigma). The antigen–antibody reactions were detected by enhanced chemiluminescence (ECL; Amersham Pharmacia) and exposed to autoradiographic film.

Immunohistochemistry. Freshly harvested mouse skin was fixed in 4% PFA and embedded in paraffin by the Comprehensive Cancer Center Immunohistochemistry Core (University of California, San Francisco). Immunofluorescence staining was performed after deparaffinization of 5-μm sections in xylene, rehydration, and antigen retrieval in 10 mM Na Citrate. The sections were washed in PBS and nonspecific antigens blocked for 30 min with 10% FCS in PBS. Proteins were bound with the rabbit anti-phospho-Smad2/3 antibody (Santa Cruz Biotechnology) and detected by using a secondary Alexa Fluor 488 anti-rabbit antibody (Molecular Probes). Slides were washed and mounted in Vectashield hard set mounting medium with DAPI (Vector Laboratories).

We thank Jonathan Yingling (Eli Lilly) for the gift of anti-phospho-SMAD2 antibody. This work was supported by National Institutes of Health Grants P01 AR050440 (to R.J.A. and A.B.), R01 GM60514 (to R.J.A.), and U01 CA84244 (to A.B.), and U.S. Department of Energy Grant DE-FG02-03ER63630 (to A.B. and J.-H.M.).

1. Akhurst, R. J. (2002) *J. Clin. Invest.* **109,** 1533–1536.
2. Muraoka, R. S., Dumont, N., Ritter, C. A., Dugger, T. C., Brantley, D. M., Chen, J., Easterly, E., Roebuck, L. R., Ryan, S., Gotwals, P. J., *et al.* (2002) *J. Clin. Invest.* **109,** 1551–1559.
3. Yang, Y. A., Dukhanina, O., Tang, B., Mamura, M., Letterio, J. J., MacGregor, J., Patel, S. C., Khozin, S., Liu, Z. Y., Green, J., *et al.* (2002) *J. Clin. Invest.* **109,** 1607–1615.
4. Cui, W., Fowlis, D. J., Bryson, S., Duffie, E., Ireland, H., Balmain, A. & Akhurst, R. J. (1996) *Cell* **86,** 531–542.
5. Derynck, R., Akhurst, R. J. & Balmain, A. (2001) *Nat. Genet.* **29,** 117–129.
6. Roberts, A. B. & Wakefield, L. M. (2003) *Proc. Natl. Acad. Sci. USA* **100,** 8621–8623.
7. Derynck, R., Goeddel, D. V., Ullrich, A., Gutterman, J. U., Williams, R. D., Bringman, T. S. & Berger, W. H. (1987) *Cancer Res.* **47,** 707–712.
8. Sieweke, M. H., Thompson, N. L., Sporn, M. B. & Bissell, M. J. (1990) *Science* **248,** 1656–1660.
9. Akhurst, R. J. & Derynck, R. (2001) *Trends Cell Biol.* **11,** S44–S51.
10. Bhowmick, N. A., Chytil, A., Plieth, D., Govska, A. E., Dumont, N., Shappell, S., Washington, M. K., Neilson, E. G. & Moses, H. L. (2004) *Science* **303,** 848–851.
11. Welch, D. R., Fabra, A. & Nakajima, M. (1990) *Proc. Natl. Acad. Sci. USA* **87,** 7678–7682.
12. Torre-Amione, G., Beauchamp, R. D., Koeppen, H., Park, B. H., Schreiber, H., Moses, H. L. & Rowley, D. A. (1990) *Proc. Natl. Acad. Sci. USA* **87,** 1486–1490.
13. Arteaga, C. L., Hurd, S. D., Winnier, A. R., Johnson, M. D., Fendly, B. M. & Forbes, J. T. (1993) *J. Clin. Invest.* **92,** 2569–2576.
14. Cambien, F., Ricard, S., Troesch, A., Mallet, C., Generenaz, L., Evans, A., Arveiler, D., Luc, G., Ruidavets, J. B. & Poirier, O. (1996) *Hypertension* **28,** 881–887.
15. Chen, T., Triplett, J., Dehner, B., Hurst, B., Colligan, B., Pemberton, J., Graff, J. R. & Carter, J. H. (2001) *Cancer Res.* **61,** 4679–4682.
16. Pasche, B., Kolachana, P., Nafa, K., Satagopan, J., Chen, Y. G., Lo, R. S., Brener, D., Yang, D., Kirstein, L., Oddoux, C., *et al.* (1999) *Cancer Res.* **59,** 5678–5682.
17. Dunning, A. M., Ellis, P. D., McBride, S., Kirschenlohr, H. L., Healey, C. S., Kemp, P. R., Luben, R. N., Chang-Claude, J., Mannermaa, A., Kataja, V., *et al.* (2003) *Cancer Res.* **63,** 2610–2615.
18. Ewart-Toland, A., Chan, J. M., Yuan, J., Balmain, A. & Ma, J. (2004) *Cancer Epidemiol. Biomarkers Prev.* **13,** 759–764.
19. Ziv, E., Cauley, J., Morin, P. A., Saiz, R. & Browner, W. S. (2001) *J. Am. Med. Assoc.* **285,** 2859–2863.
20. Hishida, A., Iwata, H., Hamajima, N., Matsuo, K., Mizutani, M., Iwase, T., Miura, S., Emi, N., Hirose, K. & Tajima, K. (2003) *Breast Cancer* **10,** 63–69.
21. Yamada, Y., Fujisawa, M., Ando, F., Niino, N., Tanaka, M. & Shimokata, H. (2002) *J. Hum. Genet.* **47,** 243–248.
22. Yokota, M., Ichihara, S., Lin, T. L., Nakashima, N. & Yamada, Y. (2000) *Circulation* **101,** 2783–2787.
23. Grainger, D. J., Heathcote, K., Chiano, M., Snieder, H., Kemp, P. R., Metcalfe, J. C., Carter, N. D. & Spector, T. D. (1999) *Hum. Mol. Genet.* **8,** 93–97.
24. Shin, A., Shu, X. O., Cai, Q., Gao, Y. T. & Zheng, W. (2005) *Cancer Epidemiol. Biomarkers Prev.* **14,** 1567–1570.
25. Nagase, H., Bryson, S., Cordell, H., Kemp, C. J., Fee, F. & Balmain, A. (1995) *Nat. Genet.* **10,** 424–429.
26. Ewart-Toland, A., Briassouli, P., de Koning, J. P., Mao, J. H., Yuan, J., Chan, F., MacCarthy-Morrogh, L., Ponder, B. A., Nagase, H., Burn, J., *et al.* (2003) *Nat. Genet.* **34,** 403–412.
27. Nagase, H., Mao, J. H., de Koning, J. P., Minami, T. & Balmain, A. (2001) *Cancer Res.* **61,** 1305–1308.
28. Fowlis, D. J., Flanders, K. C., Duffie, E., Balmain, A. & Akhurst, R. J. (1992) *Cell Growth Differ.* **3,** 81–91.
29. Yue, J. & Mulder, K. M. (2000) *J. Biol. Chem.* **275,** 35656.
30. Van Obberghen-Schilling, E., Roche, N. S., Flanders, K. C., Sporn, M. B. & Roberts, A. B. (1988) *J. Biol. Chem.* **263,** 7741–7746.
31. Bremner, R. & Balmain, A. (1990) *Cell* **61,** 407–417.
32. Kemp, C. J., Fee, F. & Balmain, A. (1993) *Cancer Res.* **53,** 6022–6027.
33. Tang, Y., Sook Lee, K., Yang, H., Logan, D. W., Wang, S., McKinnon, M. L., Holt, L. J., Condie, A., Luu, M. T. & Akhurst, R. J. (2005) *Genomics* **85,** 60–70.
34. Akhurst, R. J., Fee, F. & Balmain, A. (1988) *Nature* **331,** 363–365.
35. Cook, T., Gebelein, B., Mesa, K., Mladek, A. & Urrutia, R. T. (1998) *J. Biol. Chem.* **273,** 25929–25936.
36. Kowanetz, M., Valcourt, U., Bergström, R., Heldin, C.-H. & Moustakas, A. (2004) *Mol. Biol. Cell* **24,** 4241–4254.
37. Ota, T., Fujii, M., Sugizaki, T., Ishii, M., Miyazawa, K., Aburatani, H. & Miyazono, K. (2002) *J. Cell Physiol.* **193,** 299–318.
38. Siegel, P. M., Sku, W. & Massague, M. (2003) *J. Biol. Chem.* **12,** 35444–35450.
39. Lasorella, A., Rothschild, G., Yokota, Y., Russell, R. G. & Iavarone, A. (2000) *Nature* **407,** 592–598.
40. Benezra, R., Rafii, S. & Lyden, D. (2001) *Oncogene* **20,** 8334–8341.
41. Paris, P. L., Andaya, A., Fridlyand, J., Jain, A. N., Weinberg, V., Kowbel, D., Brebner, J. H., Simko, J., Watson, J. E., Volik, S., *et al.* (2004) *Hum. Mol. Genet.* **13,** 1303–1313.
42. Dang, C. V., O'Donnell K. A. & Juopperi, T. (2005) *Cancer Cell* **8,** 177–178.